Filling in of Fraunhofer lines by plant fluorescence: Simulations for a nadir-viewing satellite-borne instrument

Christopher E. Sioris,[1,2] Grégory Bazalgette Courrèges-Lacoste,[3] and Marc-Philippe Stoll[4]

Received 24 September 2001; revised 22 April 2002; accepted 19 November 2002; published 21 February 2003.

[1] Solar-excited plant fluorescence in the red/near-infrared is known to fill Fraunhofer lines at ground level. In this paper, it is shown that red/near-infrared fluorescence by vegetation can fill Fraunhofer lines much more effectively than rotational Raman scattering (RRS) by air (Ring effect) for nadir viewing from satellite altitudes. Thus, similarly to RRS, plant fluorescence can be remotely sensed from an orbiting spectrometer, and may impact the retrieval of atmospheric trace gases such as water vapor by high-resolution spectroscopy over vegetated land. *INDEX TERMS:* 0315 Atmospheric Composition and Structure: Biosphere/atmosphere interactions; 0649 Electromagnetics: Optics; 0933 Exploration Geophysics: Remote sensing; *KEYWORDS:* inelastic, radiative transfer

Citation: Sioris, C. E., G. Bazalgette Courrèges-Lacoste, and M.-P. Stoll, Filling in of Fraunhofer lines by plant fluorescence: Simulations for a nadir-viewing satellite-borne instrument, *J. Geophys. Res.*, *108*(D4), 4133, doi:10.1029/2001JD001321, 2003.

1. Introduction

[2] The simulations described in this paper were performed as part of the Fluorescence Explorer (FLEX) feasibility study. FLEX [*Stoll et al.*, 1999] is a proposed nadir-viewing satellite mission to demonstrate that natural fluorescence from vegetation can be measured passively and cost-effectively from space using the filling in of spectrally coincident Fraunhofer lines (see Table 1).

[3] The filling in of solar and telluric absorption lines in skylight is known as the Ring effect [*Grainger and Ring*, 1962]. *Brinkmann* [1968] established that inelastic rotational Raman scattering (RRS) by O_2 and N_2 could explain the magnitude of the observed Ring effect. At present, RRS is considered to be the dominant filling-in mechanism for all viewing geometries including satellite nadir [e.g., *Burrows et al.*, 1996; *Vountas et al.*, 1998; *Sioris and Evans*, 2000].

[4] The goal of this paper is to illustrate that the Fraunhofer filling-in effect due to plant fluorescence is comparable under clear sky conditions to that of RRS by air in the visible for nadir viewing from space. This finding is expected to be of interest to the biospheric remote sensing community, atmospheric spectroscopists mapping trace gases with satellite-borne spectrometers in the visible and near-IR, and Ring effect researchers.

[5] For FLEX, the removal of the RRS spectral signature using appropriate radiative transfer models [e.g., *Sioris and Evans*, 2002; *Sioris et al.*, 2002] is one of the necessary steps in the atmospheric correction of the observed radiance spectra. If the RRS signature is of the same order of magnitude as that of the fluorescence, the accuracy of the RRS models combined with accurate surface reflectance and aerosol information will be sufficient to allow the intensity of the fluorescence to be extracted [*Bazalgette Courrèges-Lacoste et al.*, 2001].

[6] The fluorescence of green vegetation consists of the red and far-red fluorescence (maxima at 690 and 740 nm) arising from chlorophyll pigments and of blue-green fluorescence (maxima at 440 and 520 nm). The red fluorescence signal emitted from vegetation is directly linked to the photosynthesis and as such may be used as an indicator for plant functioning, stress and vitality. In fact, the decrease of the photosynthetic activity by various types of stress makes chlorophyll fluorescence a valuable tool for characterizing the state of health of a plant [*Lichtenthaler et al.*, 1998]. The blue-green fluorescence is not related to photosynthesis, but was recently found to originate from ferulic acid and other components of the cell's membrane [*Morales et al.*, 1996; *Lichtenthaler and Schweiger*, 1998]. Nevertheless, the physics of blue-green fluorescence is complex and not fully understood. A "typical" fluorescence emission spectrum of a green leaf excited with UV/visible radiation is shown in Figure 1. However, plant fluorescence is highly variable in its intensity and spectral characteristics. The solar-excited fluorescence spectrum is known to vary as a function of the time-integrated incident radiation and the plant physiology among other predictor variables.

[7] As shown in Figure 1, plant fluorescence is spectrally broad and smooth (devoid of Fraunhofer structure) whereas the solar radiation scattered by the surface and the atmosphere contains Fraunhofer structure. In general, any background additive term to a given spectral radiance decreases the depth of the Fraunhofer lines when expressed relative to a reference free of this additional term. Thus when plant fluorescence (or any broadband emission) is significantly intense relative to other radiance sources (i.e., atmospheric

[1]Centre for Research in Earth and Space Science, York University, Toronto, Ontario, Canada.
[2]Now at Atomic and Molecular Physics Division, Harvard-Smithsonian Center for Astrophysics, Cambridge, Massachusetts, USA.
[3]Space Instrumentation Division, TNO-TPD, Delft, Netherlands.
[4]Laboratoire des Sciences de l'Image, de l'Informatique et de la Télédétection, Université Louis Pasteur, Strasbourg, France.

0148-0227/03/2001JD001321

Table 1. FWHM (nm) of Selected Fraunhofer Lines Pre- and Post-Convolution With Required Slit Function[a]

Line	λ,[b] nm	FWHM of Line	Slit FWHM	Effective FWHM of Line
Ca II H	396.85	0.884	0.14	1.13
Fe G	430.8	n/a[c]	0.0929	0.111
Hβ	486.13	0.132	0.094	0.189
Hα	656.28	0.144	0.043[d]	0.1853
Fe I	685.52	0.014	0.014	0.0158

[a]FWHM is in nm.
[b]Wavelengths were determined by high-resolution ground-based solar spectroscopy [*Moore et al.*, 1966], except for Fe G which appears as a single line only in low-resolution observations.
[c]Fe G is primarily the result of two narrow, fairly intense, closely spaced Fraunhofer lines (due to Fe and Ca) that are smeared into one deep line upon convolution.
[d]Hα is not convolved: 0.043 nm is the spectral sampling (see text for details).

and surface scattering), Fraunhofer line depths are reduced relative to the continuum as compared to line depths in the case of viewing a nonfluorescent target. In other words, the depth of Fraunhofer lines in radiance spectra observed from satellite nadir-viewing geometry depends on the intensity of the plant fluorescence relative to the intensity of the reflectance of the Earth and its atmosphere. By selecting deep Fraunhofer lines where reflected intensities are low, fluorescence can be remotely detected by passive means.

[8] Measurements of fluorescence using Fraunhofer line filling in have been made for over two decades from both ground level [e.g., *MacFarlane et al.*, 1980] and from aircraft, beginning with the pioneering work of *Plascyk* [1975] and coworkers on the Mark II Fraunhofer Line Discriminator. However, the detection of fluorescence from above the atmosphere is complicated because of the following: (1) fluorescence, much like reflectance from plants, is attenuated as it traverses the atmosphere on the way up to the satellite and (2) the atmosphere scatters sunlight up to the satellite just as the surface does. Thus, there are two sources of scattered sunlight.

[9] As a result of effect (1), fluorescence from vegetation comprises a smaller fraction of the total signal measured by a nadir-viewing satellite because this radiation is attenuated due to atmospheric scattering and absorption along the line of sight. In particular, Rayleigh scattering in the UV/blue limits the contribution of plant fluorescence to the total signal. Second (see effect 2), the atmosphere contributes much of the total nadir radiance (again especially in the UV/blue), thereby decreasing the relative contribution of fluorescence and making its detection more difficult.

[10] In order to simulate the filling in, the Moderate Resolution Transmission (MODTRAN) radiative transfer model [*Berk et al.*, 1999] is used to calculate the transmission of the fluorescence and the nadir radiance excluding fluorescence by vegetation and RRS. The Ring effect is subsequently added to the nadir radiance through the use of a RRS forward model [*Sioris et al.*, 2002].

[11] For FLEX, it is crucial that the filling in from RRS can be taken into account, so that filling in due to fluorescence can be mapped from space. The inelastic scattering is almost entirely due to rotational Raman scattering by atmospheric N_2 and O_2 and amounts to ~4% of Rayleigh scattering throughout the visible. Figure 2 shows the weak inelastic lines (due to RRS) shifted from the much stronger elastic (Rayleigh) line. Fraunhofer lines are filled in because more radiation is shifted to the wavelengths of these solar absorption features (λ) than is shifted from these wavelengths (Figure 3). In other words, there is a significant (e.g., >1%) net gain in radiance in the core of deep Fraunhofer lines. Quantitatively, filling in is defined as $(I_\lambda - J_\lambda)/J_\lambda$ where I_λ is the spectral radiance including RRS or fluorescence and J_λ is the spectral radiance excluding both filling-in mechanisms (RRS and fluorescence) from the simulation. The Ring effect depends directly on the line depth and instrument resolution. To a first approximation, the Ring effect can be visualized as a convolution of the solar spectrum with the Rayleigh band spectrum of air.

[12] Part of the FLEX feasibility study involved choosing the ideal instrument. Two designs were being considered: a grating spectrometer (moderate to high spectral resolution) and a high-resolution (quantified below) Fabry-Perot. For the grating spectrometer, simulations were performed for Fraunhofer lines and instrumental spectral resolutions listed in Table 1. Fabry-Perot (F-P) simulations were then performed for the most promising Fraunhofer line in the blue-green (i.e., Hβ) and the best candidate in the red (i.e., Fe I) based on extensive fluorescence-to-noise studies for the grating spectrometer [*Bazalgette Courrèges-Lacoste et al.*, 2001]. Lines with similar depth to Fe I (685.5 nm) at λ > 710 nm such as Fe I (~739 nm) were not considered viable alternatives because of the dramatic increase in reflectance by vegetation in the near-IR known as the red-edge. The *A* and *B* bands of O_2 are not considered because the absorp-

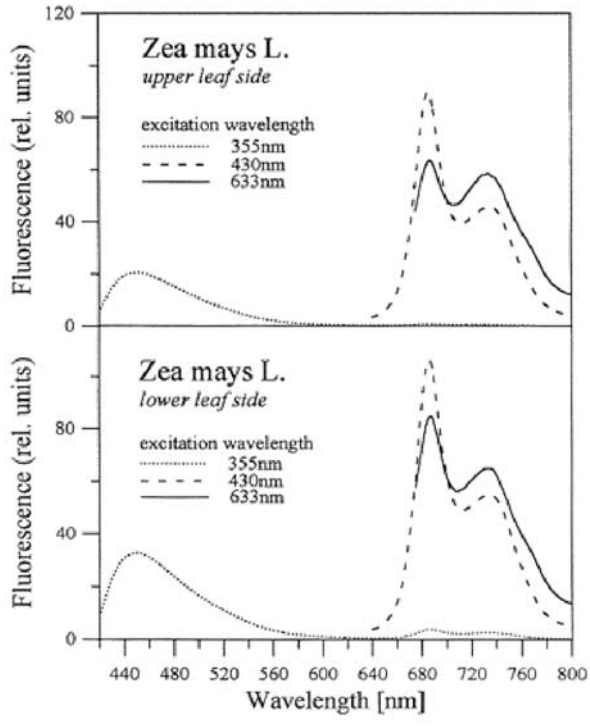

Figure 1. Fluorescence emission spectra of the upper and lower leaf side of a full-grown maize leaf (chlorophyll content 33.2 μg cm^{-2}). The chlorophyll flourescence yield is much higher for excitation at 430 nm and 633 nm than by UV radiation (355 nm) [*Lichtenthaler et al.*, 1998].

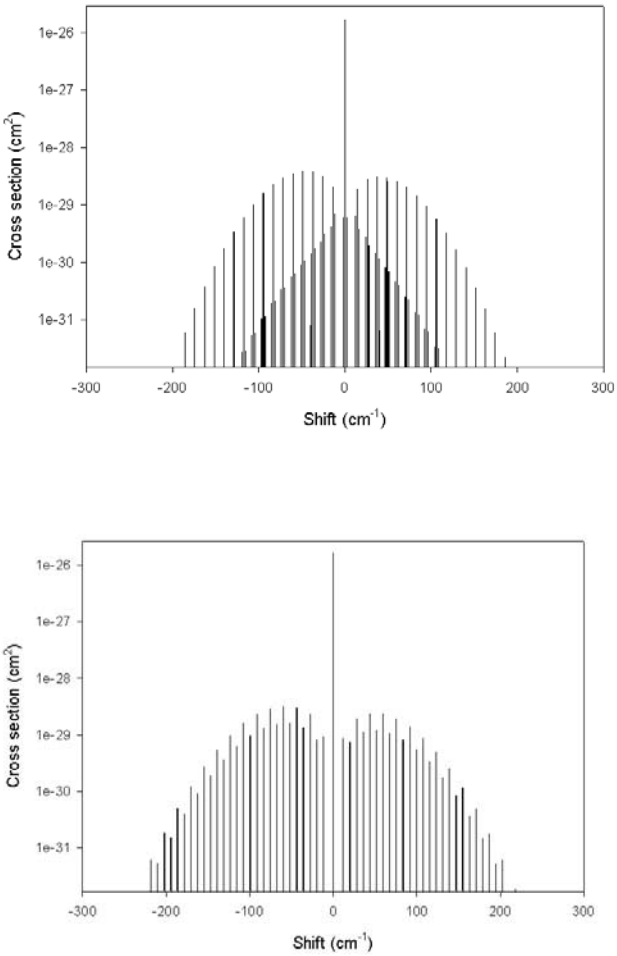

Figure 2. (a) Rayleigh band spectrum of O_2 for an excitation wavelength (λ) of 397 nm and temperature (T) of 250 K. Note the log scale in the y axis. To a first approximation, the Rayleigh scattering cross sections exhibit a λ^{-4} dependence. (b) Rayleigh band spectrum of N_2 at λ = 397 nm, T = 250 K.

tion optical thickness at these wavelengths means that fluorescence emitted from the surface cannot effectively transmit to space (see also *Carter et al.* [1996]; *Kebabian et al.* [1999]). The complexity of the radiative transfer and spectroscopy (i.e., pressure-induced line shifts, Ring effect [*Sioris and Evans*, 2000], pressure and temperature dependent line widths, temperature dependent line intensities, etc.) in these bands would also complicate any fluorescence retrieval algorithm as compared to using Fraunhofer lines. In general, for fluorescence filling in to compete with the Ring effect in terms of magnitude, the Fraunhofer lines must occur at wavelengths where the intensity of the fluorescence by vegetation and the atmospheric transmission are both high, and the Earth-atmosphere reflectance is low.

2. Choice of Model Input Parameters

[13] Since the detection of fluorescence by Fraunhofer filling in relies on the depth of the solar absorption lines, one of the key inputs into the radiance modeling is an accurate solar irradiance spectrum. Many measured solar irradiance spectra have one or more of the following shortcomings: (1) inadequate spectral resolution, (2) lack of absolute calibration of irradiance, and (3) telluric absorption.

[14] The requirements of the FLEX feasibility study dictated that none of these three limitations exist for the input solar reference spectrum. The high spectral resolution was required for the Fabry-Perot simulations of Hβ and Fe I and the Fe I grating spectrometer simulation in order to adequately resolve the line core for fluorescence detection. The high spectral resolution was also of interest because the filling in due to RRS has a direct, exponential dependence on instrumental spectral resolution [*Sioris et al.*, 2002], which is stronger than the resolution dependence of fluorescence filling in as will be illustrated below. Thus the high-resolution case would provide the ultimate confirmation that fluorescence can fill in Fraunhofer lines comparably to RRS for nadir viewing. The absolute calibration of the incoming solar irradiance was required only because one of the goals for FLEX is to retrieve the absolute zenith fluorescent radiance at ground level due to vegetation. However, the absolute calibration is not specifically necessary in this modeling experiment.

[15] The "New Kurucz" solar spectrum [*Kurucz*, 1995a, 1995b] in MODTRAN4 [*Berk et al.*, 1999] does not contain telluric features since absorbing spectral regions (i.e., O_2A band) are replaced with a synthetic solar irradiance calculated at very high resolution [*Kurucz*, 1992a, 1992b, and references therein]. The spectral irradiance is subsequently binned in 1-cm^{-1} increments. However, the Fe I line at ~685.5 nm has a full width at half maximum (FWHM) of ~12 pm. Thus, this narrow line will not be resolved since 1 cm^{-1} = 47 pm at Fe I. However, MODTRAN can still be used to calculate the radiance due to elastic scattering assuming the fine structure in the nadir spectral radiance at Fe I is due to solar features only. In this case, sun-normalized MODTRAN4 nadir spectral radiances for a variety of atmospheric scenarios have been applied to appropriate solar irradiance spectra. For the grating spec-

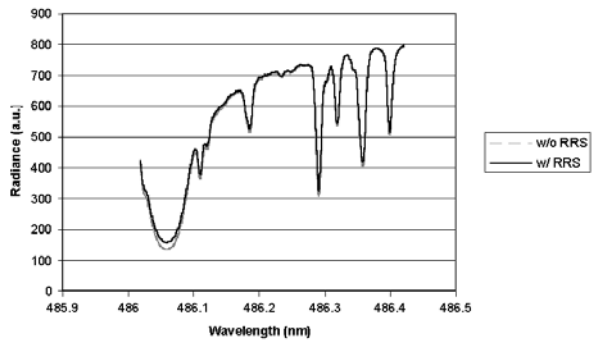

Figure 3. Spectral radiance in the vicinity of Hβ (486.1 nm) profile simulated with and without inelastic scattering (solar zenith angle of 60°, nadir viewing, no aerosols, no gaseous absorption, no albedo (A = 0), sampling = 0.01 cm^{-1} (0.0002 nm), resolution = 0.026 cm^{-1} (0.0006 nm), T = 248 K and solar spectrum from *Beckers et al.* [1976]).

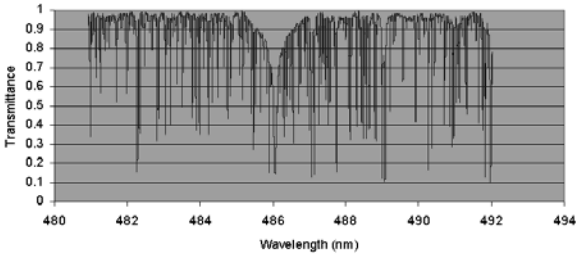

Figure 4. Transmission spectrum near Hβ (481.0–492.0 nm) from the photosphere to 2.8 km above Earth's surface (at Sacramento Peak, New Mexico) with a spectral resolution of 0.026 cm^{-1} or 0.0006 nm at Hβ [*Beckers et al.*, 1975].

trometer simulations of Hα, Hβ, Fe G, Ca II H, the solar irradiance spectrum in MODTRAN4 is adequate.

[16] Rocket and satellite-borne spectrometers have yet to measure the visible spectral region at the resolution required for the F-P simulations. Measured solar spectra from the ground [e.g., *Beckers et al.*, 1976] and from balloons can provide the necessary resolution, but inevitably include telluric absorption. *Beckers et al.* [1976] recorded a disk-integrated high-resolution solar irradiance spectrum (see Figure 4), and then removed broadband features from the spectrum (Rayleigh and Mie scattering, broadband absorption, and the solar Planck function). This normalized irradiance spectrum was converted to an absolutely calibrated irradiance scale by dividing the entire spectrum by the irradiance at the wavelength of minimum absorption to obtain a % transmission through the solar atmosphere. Then, this transmittance spectrum is multiplied by a Planck curve (at ~5800 K) to yield an approximation of the solar irradiance spectrum adequate for modeling of radiance including fluorescence and RRS filling in.

[17] Water vapor polyads lead to telluric features in the vicinity of the Fe line (685.5 nm) in the Beckers et al. spectrum. This absorption signature is extremely weak and fortunately does not overlap the Fe I line even when pressure broadening of these H_2O lines by air at 1 atm is considered. For the inelastic scattering calculations, even absorption lines in the vicinity of the Fraunhofer line will reduce the accuracy of the calculation as radiation is shifted from the nearby continuum into the line. This is particularly important for Fe I because of the proximity of the *B* band of O_2 (~687 nm). The erroneous presence of this strong telluric band in the solar spectrum slightly reduces the magnitude of the simulated Ring effect. The magnitude of this error was quantified for the Fabry-Perot by linearly interpolating over the *B* band to remove this feature (and underlying Fraunhofer lines). Then, the radiance (including RRS) was recalculated at Fe I. The net gain in radiance due to the inelastic scattering averaged over the FW of the instrumental transmission function increased by 21% (i.e., the Ring effect was 1.21 times greater than prior to interpolating over the *B* band). Further details are given below.

[18] The solar irradiance spectrum is just one of the inputs to the radiative transfer modeling. Other important parameters such as instrumental spectral resolution are discussed hereafter. For the grating spectrometer simulations, the minimum resolution (FWHM of the instrument function) required is the FWHM of the Fraunhofer line as determined from a high-resolution solar atlas [e.g., *Beckers et al.*, 1976] for all selected lines except for Hα, where the minimum resolution appropriate for FLEX is 0.06 nm [*Stoll et al.*, 1999]. A boxcar function was used for the instrumental profile, except for Ca II H where a triangular slit function was used and Hα, where the spectrum is at ultrahigh resolution but binned in 1-cm^{-1} increments (not convolved). After convolution with the slit function, the apparent FWHM of a Fraunhofer line increases. The extent of the increase in FWHM of the line due to the convolution depends directly on the FWHM of the slit function (see Table 1). The radiance is calculated over the apparent FWHM of each line.

[19] For the F-P simulations, the radiance including RRS is calculated for spectral bandpasses of 4.1 and 50 pm at the line centers of Fe I and Hβ, respectively.

[20] To investigate the impact of atmospheric haze, two aerosol models were initially chosen for the lower atmosphere and two for the stratosphere (upper atmosphere). The two stratospheric aerosol models were (1) background stratospheric profile and extinction and (2) moderate volcanic profile, background stratospheric extinction.

[21] The latter aerosol model would help determine the feasibility of FLEX in the aftermath of a volcano. It was quickly realized after the first few simulations that the decreased transmission of fluorescence and increased backscattering due to an increase in stratospheric aerosol loading (i.e., a couple of years after a major volcano) would not significantly reduce the top-of-the-atmosphere nadir fluorescence. Thus, all subsequent simulations included background stratospheric aerosol concentrations.

[22] For the lower atmosphere, where most of the aerosol burden is located, two aerosol models were selected: (1) boundary layer aerosol typical of a rural setting (visibility = 23 km) and (2) a clean boundary layer (visibility = 50 km).

[23] Aerosol phase functions are computed from Mie scattering theory and a two-stream approximation is used.

[24] The model atmosphere was the 1976 U.S. Standard. No clouds were included. The surface was considered to be at sea level.

[25] For radiance simulations, two additional parameters are required: surface spectral albedo (A) and solar zenith angle (SZA). Two SZAs were chosen: 30° and 60°. Different surfaces were chosen so as to investigate the impact of brighter and darker types of vegetation. Some examples are black spruce [*Sampson et al.*, 1998], young corn [*Suits and Safir*, 1972], and cottonwood [*Henderson-Sellers and Robinson*, 1994]. Lambertian surface reflectance is assumed.

[26] A detailed description of the Raman scattering model is available elsewhere [*Sioris et al.*, 2002] and recently updated spectroscopic parameters [*Sioris and Evans*, 2000] have been included. For the grating spectrometer simulations, the spectral radiance is interpolated onto a 1-cm^{-1} grid and all Raman shifts are executed to the nearest cm^{-1}, except for Fe I, for which a 0.01-cm^{-1} grid is required and, consequently, the Raman line positions are rounded to the nearest hundredth of a wave number. For the Fabry-Perot simulations, a 0.01-cm^{-1} grid was also used. An isothermal atmosphere at 248 K was assumed for the calculation of the RRS cross sections. Collisional broadening of the RRS lines [*Burrows et al.*, 1996] and Brillouin scattering by air is

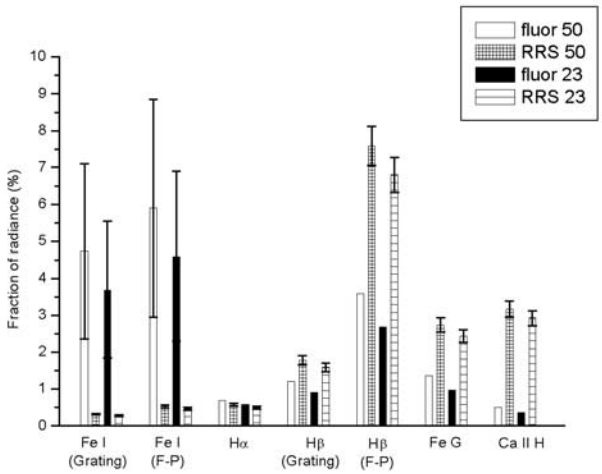

Figure 5. Fluorescence (abbreviated "fluor" in the legend) and RRS as% of total radiance averaged over FWHM of Fraunhofer line (for grating) and over FW of instrumental transmission function (for F-P) (SZA = 60°, 1976 U.S. Standard atmosphere, $0.02 \leq A \leq 0.05$, where A is the surface albedo and is assumed to be Lambertian). The numbers in the legend are the visibilities in kilometers. Simulations are for a grating spectrometer unless indicated otherwise. Uncertainties are discussed in the text.

neglected since the half widths at half maximum of these phenomena are about an order of magnitude narrower than even the narrowest Fraunhofer line (i.e., Fe I) and thus neither of these would change the filling in significantly. Brillouin and Rayleigh wing scattering by vegetation are not included although they represent additional filling-in mechanisms at high resolution for backscattering geometries and require experimental investigation. Vibrational Raman scattering by plants or water contained in the plants is at least six orders of magnitude weaker than fluorescence and need not be considered [*Schrader et al.*, 1999].

[27] The exoatmospheric fluorescence radiance is the canopy-level fluorescence irradiance divided by π and multiplied by the atmospheric transmittance. Fluorescence irradiance values are based on estimates of fluorescence with solar excitation [*Goulas*, 1992].

3. Results, Conclusions and Future Work

[28] The filling-in simulations (Figure 5) use the spectral albedo for cottonwood tree (*Populus deltoides*) [*Henderson-Sellers and Robinson*, 1994] except for Fe G, where an albedo of 0.02 was assumed, appropriate for young corn [*Suits and Safir*, 1972]. The filling in due to fluorescence is of the same order of magnitude as the filling in due to RRS for FLEX geometry (nadir-viewing) and lines in the visible except Fe I. At Fe I, the filling in by fluorescence is approximately one order of magnitude larger than that by RRS for both the Fabry-Perot and grating spectrometer.

[29] The large error bars on the simulated fluorescence filling in are almost entirely due to the uncertainty of the fluorescence irradiance estimates. This is to be expected to due the intrinsic variability and complexity of this phenomenon. A crude estimate of the variability of blue-green fluorescence by green vegetation is a factor of 20 [*Goulas*, 1992]. The fluorescence at Hα varies by roughly two orders of magnitude due to stress alone [*Watson et al.*, 1973]. The value conservatively assumed in our simulation was 0.2 mW/m^2/nm [*Goulas*, 1992], but as high as 6 mW/m^2/nm has been observed elsewhere [*Carter et al.*, 1990]). The variability is partly explained by the spectral gradient in the fluorescence at 656 nm (see Figure 1). The uncertainties are considerably smaller at Fe I (685.5 nm), which lies near the peak of the RF. Values between 1.2 and 3 mW/m^2/nm [*Kebabian et al.*, 1999] were observed at the O_2B band a few nanometers long of Fe I. This range encompasses the value assumed for Fe I in this study: 2 mW/m^2/nm [*Goulas*, 1992]. The error on the filling in due to RRS is much smaller and is dominated by approximations in the atmospheric radiative transfer as the measured [e.g., *Penney et al.*, 1974] and modeled RRS cross sections (Figure 2) of N_2 and O_2 agree to 0.4% and 2%, respectively, and the line positions are known to 0.002 cm^{-1} [e.g., *Rothman et al.*, 1998]. The agreement between the conservative Raman scattering model used here [*Sioris et al.*, 2002] and SCIATRAN (formerly GOMETRAN-RRS) [*Vountas et al.*, 1998] was 2% for a nadir clear-sky case [*de Beek et al.*, 2001] with a visibility of 50 km, A = 0.05 (ocean), and SZA = 32° at Ca II K and GOME-FM resolution while SCIATRAN and GOME-FM Ring effect measurements consistently agree to ±7% for most clear sky cases.

[30] Assuming these fluorescence irradiance estimates are realistic, only models that include both filling-in phenomena can simulate the magnitude of the filling in for these types of cases. The simulations also show that the fraction of the total radiance due to fluorescence decreases more sharply with increasing boundary layer aerosol loading than the RRS contribution to the radiance (Figure 5). RRS also dominates over fluorescence for deeper lines (or higher spectral resolutions) and toward shorter wavelengths.

[31] Because the filling in due to fluorescence has a different dependence on line depth than that due to RRS, the spectral structure introduced by these two mechanisms is not completely correlated. Thus, fitting a Ring spectrum [e.g., *Vountas et al.*, 1998] will not completely remove the fluorescence signature and may impact retrieval of NO_2 from the 450-nm region. Furthermore, if the NO_2 fitting region is wide enough, the different wavelength dependences of the two effects will also complicate the removal of the filling in by a single Ring spectrum. Nevertheless, the pseudo-absorber approach to the Ring effect correction will actually work quite well simply because of the partial correlation between RRS and fluorescence filling in.

[32] However, alternative approaches which do not let the Ring correction be freely scalable in magnitude, such as the backward Ring effect correction model [*Sioris et al.*, 2002], will not remove any the filling in of Fraunhofer lines due to plant fluorescence. Completely neglecting the Ring effect can result in an overestimation of the vertical column density of NO_2 for GOME by 8.5% at SZA = 30° using the 420- to 460-nm fitting window [*Vountas et al.*, 1998]. Thus, similar errors would be expected for neglecting fluorescence in the same spectral region. The RF overlaps with a fitting window previously used for retrieval of water vapor [*Noël et al.*, 1999].

[33] It would be interesting to see if the filling in of Hβ over vegetated land is greater than over other surfaces with similar reflectivity by analyzing GOME data. GOME only has a spectral resolution of ~0.3 nm in the visible [*Aben et al.*, 1997] and filling-in observations in the visible over land by this or any other nadir-viewing exoatmospheric spectrometer have yet to be quantitatively analyzed.

[34] In conclusion, the need for further measurements of solar-excited plant fluorescence irradiance spectra, particularly in the blue-green, is clear.

[35] **Acknowledgments.** The authors would like to acknowledge I. Moya (Université de Paris-Sud) for providing the fluorescence irradiance data from the Goulas thesis and C. Buschmann for providing Figure 1 and for valuable discussions regarding fluorescence by vegetation.

References

Aben, I., F. Helderman, D. M. Stam, and P. Stammes, High-spectral resolution polarisation measurements of the atmosphere with the GOME BBM, *Proc. SPIE*, *3121*, 446–453, 1997.

Bazalgette Courrèges-Lacoste, G., A. Court, C. Smorenburg, H. Visser, M.-P. Stoll, and K. Buschmann, FLEX instrument feasibility study, final report, *ESA contract 14385/00/NL/DC*, 108 pp., TNO-TPD, Delft, Netherlands, 2001.

Beckers, J. M., L. Dickson, and R. S. Joyce, Observing the Sun with a fully tunable Lyot-Ohman filter, *Appl. Opt.*, *14*, 2061–2066, 1975.

Beckers, J. M., C. A. Bridges, and L. B. Gilliam, Sacramento Peak Observatory Project 7649, in *A High Resolution Spectral Atlas of the Solar Irradiance From 380 to 700 Nanometers*, vol. I, *Tabular Form*, Air Force Geophys. Lab., Hanscom AFB, Mass., 1976.

Berk, A., G. P. Anderson, P. K. Acharya, J. H. Chetwynd, L. S. Bernstein, E. P. Shettle, M. W. Matthew, and S. M. Adler-Golden, *MODTRAN4 User's Manual*, software manual, Air Force Res. Lab., Space Vehicles Dir., Air Force Mater. Command, Hanscom AFB, Mass., 1999.

Brinkmann, R. T., Rotational Raman scattering in planetary atmospheres, *Astrophys. J.*, *154*, 1087–1093, 1968.

Burrows, J., M. Vountas, H. Haug, K. Chance, L. Marquard, K. Muirhead, U. Platt, A. Richter, and V. Rozanov, Study of the Ring effect, *Tech. Rep. ESA contract 10996/94/NL/CN*, Eur. Space Agency, Noordwijk, Netherlands, 1996.

Carter, G. A., A. F. Theisen, and R. J. Mitchell, Chlorophyll fluorescence measured using the Fraunhofer line-depth principle and relationship to photosynthetic rate in the field, *Plant Cell Environ.*, *13*, 79–83, 1990.

Carter, G. A., J. H. Jones, R. J. Mitchell, and C. H. Brewer, Detection of solar-excited chlorophyll a fluorescence and leaf photosynthetic capacity using a Fraunhofer line radiometer, *Remote Sense. Environ.*, *55*, 89–92, 1996.

de Beek, R., M. Vountas, V. V. Rozanov, A. Richter, and J. P. Burrows, The Ring effect in the cloudy atmosphere, *Geophys. Res. Lett.*, *28*, 721–724, 2001.

Goulas, Y., Télédétection de la fluorescence des couverts végétaux: Temps de vie de la fluorescence chlorophylienne et fluorescence bleue, Ph.D. thesis, Université de Paris-Sud, 1992.

Grainger, J. R., and J. Ring, Anomalous Fraunhofer line profiles, *Nature*, *193*, 762, 1962.

Henderson-Sellers, A., and P. J. Robinson, *Contemporary Climatology*, 329 pp., Longman Sci. & Tech., Essex, UK, 1994.

Kebabian, P. L., A. F. Theisen, S. Kallelis, and A. Freedman, A passive two-band sensor of sunlight-excited plant fluorescence, *Rev. Sci. Instrum.*, *70*, 4386–4393, 1999.

Kurucz, R. L., "Finding" the "missing" solar ultraviolet opacity, *Rev. Mex. Astron. Astrofis.*, *23*, 181–186, 1992a.

Kurucz, R. L., Remaining line opacity problems for the solar spectrum, *Rev. Mex. Astron. Astrofis.*, *23*, 187–194, 1992b.

Kurucz, R. L., The solar irradiance by computation, in *Proceedings of the 17th Annual Review Conference on Atmospheric Transmission Models*, *PL/-TR-95-2060, Spec. Rep. 274, Pl. 332*, edited by G. P. Anderson, R. H. Picard, and J. H. Chetwynd, Phillips Lab./Geophys. Dir., Hanscomb AFB, Mass., 1995a.

Kurucz, R. L., The solar spectrum: Atlases and line identifications, in *Laboratory and Astronomical High Resolution Spectra*, *Astron. Soc. Pac. Conf. Ser.*, vol. 81, pp. 17–31, Astron. Soc. of Pacific, San Francisco, Calif., 1995b.

Lichtenthaler, H. K., and J. Schweiger, Cell wall bound ferulic acid, the major substance of the blue-green fluorescence emission of plants, *J. Plant Physiol.*, *152*, 272–282, 1998.

Lichtentaler, H. K., O. Wenzel, C. Buschmann, and A. A. Gitelson, Plant stress detection by reflectance and fluorescence, *Ann. N. Y. Acad. Sci.*, *851*, 271–285, 1998.

McFarlane, J. C., R. D. Watson, A. F. Theisen, R. D. Jackson, W. L. Ehrler, P. J. Pinter Jr., S. B. Idso, and R. J. Reginato, Plant stress detection by remote measurement of fluorescence, *Appl. Opt.*, *19*, 3287–3289, 1980.

Moore, C. E., M. G. J. Minnaert, and J. Houtgast, *The solar spectrum: 2935 Å to 8770 Å: Second revision to Rowland's preliminary table of solar spectrum wavelengths*, *Monogr. 61*, U.S. Dep. of Commer., Natl. Bur. of Stand., Washington, 1966.

Morales, F., Z. G. Cerovic, and I. Moya, Time resolved blue-green fluorescence of sugar beat (*Beta vulgaris* L.) leaves. Spectroscopic evidence for the presence of ferulic acid as the main fluorophore of the epidermis, *Biochim. Biophys. Acta*, *1273*, 251–262, 1996.

Noël, S., M. Buchwitz, H. Bovensmann, R. Hoogen, and J. P. Burrows, Atmospheric water vapour amounts retrieved from GOME satellite data, *Geophys. Res. Lett.*, *26*, 1841–1844, 1999.

Penney, C. M., R. L. St. Peters, and M. Lapp, Absolute rotational Raman cross sections for N_2, O_2, and CO_2, *J. Opt. Soc. Am.*, *64*, 712–716, 1974.

Plascyk, J. A., The MK II Fraunhofer line discriminator (FLD-II) for airborne and orbital remote sensing of solar-stimulated luminescence, *Opt. Eng.*, *14*(4), 339–346, 1975.

Rothman, L. S., et al., The HITRAN molecular spectroscopic Database and HAWKS (HITRAN Atmospheric Workstation): 1996 Edition, *J. Quant. Spectrosc. Radiat. Transfer*, *60*, 665–710, 1998.

Sampson, P. H., G. H. Mohammed, S. J. Colombo, T. L. Noland, J. R. Miller, and P. J. Zarco-Tejada, Bioindicators of forest sustainability: Progress report, *For. Res. Inf. Pap. 142*, Ont. For. Res. Inst., Minist. of Nat. Resour., Sault Ste. Marie, Ont., Canada, 1998.

Schrader, B., B. Dippel, I. Erb, S. Keller, T. Löchte, H. Schulz, E. Tatsch, and S. Wessel, NIR Raman spectroscopy in medicine and biology: Results and aspects, *J. Mol. Struct.*, *480*, 21–32, 1999.

Sioris, C. E., and W. F. J. Evans, Impact of rotational Raman scattering in the O_2A band, *Geophys. Res. Lett.*, *27*, 4085–4088, 2000.

Sioris, C. E., and W. F. J. Evans, Modeling higher order radiation fields using iterated integrals of phase functions, *J. Quant. Spectrosc. Radiat. Transfer*, *72*, 227–236, 2002.

Sioris, C. E., W. F. J. Evans, R. L. Gattinger, I. C. McDade, D. A. Degenstein, and E. J. Llewellyn, Ground-based Ring effect measurements with the OSIRIS DM, *Can J. Phys.*, *80*, 483–491, 2002.

Stoll, M.-P., A. Court, K. Smorenburg, H. Visser, L. Crocco, J. Heilimo, and A. Honig, FLEX-Fluorescence Explorer, *Proc. SPIE*, *3868*, 487–494, 1999.

Suits, G. H., and G. R. Safir, Verification of a reflectance model for mature corn with applications to corn blight detection, *Remote Sens. Environ.*, *2*, 183–192, 1972.

Vountas, M., V. V. Rozanov, and J. P. Burrows, Ring effect: Impact of rotational Raman scattering in Earth's atmosphere, *J. Quant. Spectrosc. Radiat. Transfer*, *60*, 943–961, 1998.

Watson, R. D., W. R. Hemphill, and T. D. Hessin, Quantification of the luminescent intensity of natural materials, *Proc. Am. Soc. Photogramm.*, 364–371, 1973.

G. Bazalgette Courrèges-Lacoste, Space Instrumentation Division, TNO-TPD, Delft, Netherlands. (bazalgette@tpd.tno.nl)

C. E. Sioris, Centre for Research in Earth and Space Science, York University, Toronto, Ontario, Canada. (csioris@nimbus.yorku.ca)

M.-P. Stoll, Laboratoire des Sciences de l'Image, de l'Informatique et de la Télédétection, Université Louis Pasteur-Strasbourg I, Strasbourg, France. (mpstoll@sepia.u-strasbg.fr)